The Astrophysical Journal, 647:573–586, 2006 August 10


# TROJAN PAIRS IN THE HD 128311 AND HD 82943 PLANETARY SYSTEMS?

Krzysztof Goździewski
Toruń Centre for Astronomy, Nicolaus Copernicus University, Gagarina 11, 87-100 Toruń, Poland; k.gozdziewski@astri.uni.torun.pl

and

Maciej Konacki
Nicolaus Copernicus Astronomical Center, Polish Academy of Sciences, Rabiańska 8, 87-100 Toruń, Poland; maciej@ncac.torun.pl
Department of Geological and Planetary Sciences, California Institute of Technology, MS 150-21, Pasadena, CA 91125
*Received 2005 October 5; accepted 2006 April 21*

## ABSTRACT

Two nearby stars, HD 128311 and HD 82943, are believed to host pairs of Jupiter-like planets involved in a strong first-order 2:1 mean motion resonance (MMR). In this work, we reanalyze available radial velocity (RV) measurements and demonstrate that it is also possible to explain the observed RV variations of the parent stars as being induced by a pair of Trojan planets (i.e., in a 1:1 MMR). We show that these Trojan configurations reside in extended zones of stability in which such systems can easily survive in spite of the large masses of the planets, large eccentricities, and nonzero mutual inclinations of their orbits. We also show that HD 82943 could harbor a previously unknown third planet of $\sim 0.5 M_J$ in $\sim 2$ AU orbit.

*Subject headings:* celestial mechanics — methods: *n*-body simulations — methods: numerical — planetary systems — stars: individual (HD 82943, HD 128311) — stellar dynamics

*Online material:* color figures

## 1. INTRODUCTION

Follow-up radial velocity (RV) observations of Sun-like stars with planets have revealed a number of extrasolar multiplanet systems. Many of them are involved in low-order mean motion resonances (MMRs). In particular, at least four extrasolar systems are involved in a strong first-order 2:1 MMR: Gliese 876 (Marcy et al. 2001), HD 82943 (Mayor et al. 2004), HD 128311 (Vogt et al. 2005), and HD 73526 (Tinney et al. 2006). A considerable effort has been devoted to study the origin (Kley 2003; Kley et al. 2004) and dynamical stability of these intriguing systems (e.g., Goździewski & Maciejewski 2001; Lee & Peale 2002; Ji et al. 2003; Beaugé & Michtchenko 2003; Lee 2004; Psychoyos & Hadjidemetriou 2005; Ferraz-Mello et al. 2005; Lee et al. 2006). Yet dynamical studies of the resonant configurations often rely on the two-planet Keplerian coplanar fits by the discovery teams. It has been demonstrated that the two-planet Keplerian models can be of very limited use for systems involved in strong mutual interactions (e.g., Laughlin & Chambers 2001; Rivera & Lissauer 2001; Goździewski et al. 2005). Even if a model incorporates mutual interactions, due to a typically short time span and a limited number of observations, the orbital inclinations are barely constrained, and usually only coplanar, edge-on configurations are considered. However, the recent results of Thommes & Lissauer (2003) and Adams & Laughlin (2003) suggest that a significant fraction of planetary systems involving giant planets may be substantially non-coplanar. Dynamical mechanisms that lead to fast amplification of the relative inclination are especially effective in the first-order resonance configurations (Thommes & Lissauer 2003). Also, dynamical relaxation and collisional scattering of the protoplanets may favor large relative inclinations in such systems, even if they initially emerge in a flat protoplanetary disk.

The interpretation of the RV data for multiplanet systems may be difficult. The determination of the number of planets and their orbital periods can be problematic for some systems, in particular, for those involved in a 1:1 MMR. A periodogram of the RV signal for such a system (Laughlin & Chambers 2002) is basically indistinguishable from that of a single planet in an eccentric orbit or, as we show in this paper, from a periodogram of a 2:1 MMR orbital configuration. Laughlin & Chambers (2002) and Nauenberg (2002) have demonstrated that a coplanar 1:1 MMR of Jovian planets may be stable in a wide range of their orbital parameters. The results of hydrodynamic simulations by Laughlin & Chambers (2002) indicate that Trojan planets in tadpole or horseshoe orbits might readily form and migrate within a protoplanetary disk. Presumably, a 1:1 configuration may also emerge as a result of dynamical relaxation or migration frequently used to explain 2:1 MMR configurations. In the solar system, there exist a number of moons involved in this type of resonance: the famous Janus-Epimetheus system (co-orbital moons of Saturn, exchanging orbits), Helene-Polydeuces (Trojans of Dione, a moon of Saturn), and Telesto-Calypso (Trojan moons of Tethys, yet another moon of Saturn). Dynamically, these configurations mimic planetary systems in the 1:1 MMR.

In this paper, we perform an independent analysis of the RV data for HD 128311 and HD 82943 to verify whether the observed RV variations can be explained, not only by a configuration in a 2:1 MMR, but also by 1:1 MMR. The inevitable problem with modeling such systems is that, due to a limited number of data and relatively large measurement errors, the best-fit orbital elements often and easily lead to catastrophically unstable configurations. In order to solve this problem, one needs a method of fitting that incorporates a stability criterion. Without such a constraint, one can find a stable best-fit orbit basically by chance. When we deal with a 1:1 MMR configuration, an appropriate stability control is essential, as the planets share the same (or a very similar) orbit, and a multiparameter dynamical model is highly nonlinear. In this paper we use the term "Trojan planets" not only for tadpole, close to coplanar, and circular configurations,

but for all configurations characterized by a 1:1 MMR, thus having not only similar semimajor axes but also (possibly) large relative inclinations and variable eccentricities.

## 2. NUMERICAL APPROACH

Due to strong mutual interactions, the planetary systems with giant planets have to avoid the unstable zones of the MMRs, a proximity of the collision zone and the zone of global instability where the overlapping of MMRs occurs. Otherwise, the chaotic diffusion quickly leads to collisions between the planets or with the parent star. The overall picture of the phase space of a planetary system is predicted by the fundamental Kolmogorov-Arnold-Moser theorem (Arnold 1978): the phase space is not continuous with respect to the stability criterion. Hence, commonly used (in particular, gradient-like) algorithms for exploring the phase space are poorly designed for this task because they are "blind" to a sophisticated fractal-like structure of the phase space.

The KAM stability is described in terms of stable (regular, quasi-periodic) and unstable (chaotic) motions. At first, the use of such a formal criterion in the fitting process may be problematic. Almost any planetary system, including our own, can be very close to a chaotic state. Nevertheless, we expect that even if chaos appears, it should not impair the astronomical stability (Lissauer 1999), meaning that a system is bounded over a very long time, and collisions or ejections of planets do not occur. However, for configurations involving Jupiter-like companions in close orbits with large eccentricities, the formal stability seems to be well related to the astronomical stability of the system, i.e., chaotic motions mean a fast destabilization of a planetary configuration over a short timescale related to the most significant, low-order MMRs. It has already been demonstrated by dynamical analysis of systems residing in the regions of the phase space, where the low-order MMRs are possible (e.g., Goździewski & Maciejewski 2001; Goździewski et al. 2005, 2006). We should note that there is no known general relation between the Lyapunov time (a characteristic timescale of the formal instability) and the event time (the time after which a physical change of a planetary system happens; see, e.g., Lecar et al. 2001; Michtchenko & Ferraz-Mello 2001). To put these ideas into action and to search for stable best-fit solutions in a self-consistent and optimal fashion, we treat the dynamical behavior (in terms of chaotic and regular or mildly chaotic states) as an additional observable at the same level of importance as the RV measurements. This powerful approach has already been described in detail and successfully applied in Goździewski et al. (2003, 2005, 2006).

The kernel of our approach is the genetic algorithm scheme (GA) implemented by Charbonneau (1995) in his publicly available code PIKAIA.[1] The GAs are ideal for our purpose because of their global nongradient nature and their proven ability to efficiently explore a multidimensional, noncontinuous parameter space. The RV data are modeled by a synthetic signal of the full $N$-body dynamics (Laughlin & Chambers 2001). The $(\chi^2_\nu)^{1/2}$ function is modified by a stability-penalty term employing an efficient fast indicator MEGNO (Goździewski et al. 2003). The GA fits are finally refined by yet another very accurate nongradient minimization scheme by Nelder and Mead (Press et al. 1992), widely known as the simplex method. This greatly reduces the CPU usage. We give the algorithm the acronym GAMP (genetic algorithm with MEGNO penalty).

The simplex method finds local minima of $(\chi^2_\nu)^{1/2}$. The code may also be trapped in resonance islands surrounded by strongly chaotic motions, even if $(\chi^2_\nu)^{1/2}$ inside such islands is larger than in the neighboring (but unstable) areas. By collecting solutions to which the GAMP converged in many independent runs, we gather an ensemble of the local best-fit solutions. It helps us to illustrate the multidimensional properties of $(\chi^2_\nu)^{1/2}$ and to obtain realistic estimates of the parameter's errors by choosing the solutions within prescribed limits of the overall best fit $(\chi^2_\nu)^{1/2}$ found in the entire search. At the end, some of the selected best fits can be refined with longer integration times and much lower simplex tolerance than is used during the search phase.

Finally, the stability of the best-fit solutions is examined in planes of selected orbital osculating elements using the spectral number method (SN) by Michtchenko & Ferraz-Mello (2001). It is an efficient, fast indicator completely independent of MEGNO. This enables us to verify and illustrate the best-fit solutions in a robust way and to examine dynamical properties of such configurations in wide ranges of neighboring initial conditions. Note that the SN is related here to the short-term dynamics. Thus the spectral signal analyzed is a time series $\{f(t) = a(t)\exp[\imath\lambda(t)]\}$, where $a(t)$ and $\lambda(t)$ are, respectively, an osculating *canonical* semimajor axis and longitude of a planet. Such an analysis makes it possible to resolve the proper mean motion $n$ as one of the fundamental frequencies of the system. Note also that a stability criterion in the GAMP code may be basically arbitrary. We use the formal KAM criterion as the most general and well defined.

## 3. HD 128311

HD 128311 is an active K0 star (Vogt et al. 2005). In the discovery paper, Butler et al. (2003) found an indication of a Jovian planet and a linear trend in the RV data. They concluded that, due to photospheric activity ($\log R'_{HK} \simeq -4.4$), the stellar jitter is large ($\sim$20 m s$^{-1}$), and the signal variability may be explained exclusively by the jitter. Using an updated set of 76 RV measurements, Vogt et al. (2005) found that the observations can be modeled by a system of two Jupiter-like planets involved in a 2:1 MMR. The current estimate of the stellar jitter by these authors is $\sim$9 m s$^{-1}$, but still uncertain with a 50% error. We rescale the measurement errors by adding this estimate in quadrature to the formal RV errors.

The discovery team reports that the best-fit two-planet Keplerian model yielding $(\chi^2_\nu)^{1/2} = 1.86$ and an rms $\sim$18 m s$^{-1}$ is catastrophically unstable. Using our hybrid GA/simplex code (Goździewski & Migaszewski 2006) driven by the Keplerian model of the RV, we found a different, apparently better two-planet solution that has $(\chi^2_\nu)^{1/2} = 1.717$ and an rms =15.16 m s$^{-1}$. The model parameters $(K, P, e, \omega, T_p - T_0)$, i.e., the semi-amplitude, orbital period, eccentricity, argument of periastron, and time of periastron passage for this fit are (51.948 m s$^{-1}$, 459.870 days, 0.362, 59.°401, 2474.867 days) and (77.214 m s$^{-1}$, 917.371 days, 0.248, 5.°541, 2310.806 days) for the inner and outer planet, respectively; $T_0 =$ JD 2,450,000 and the velocity offset $V_0 =$ 1.011 m s$^{-1}$. It is argued that the fit parameters of a multiplanet system should be interpreted in terms of osculating Keplerian elements and minimal masses related to the Jacobi coordinates (Lee & Peale 2003). Adopting the date of the first observation as the osculating epoch, we recalculated the inferred *astrocentric* osculating elements ($m_p \sin i, a, e, \omega, M$) as (1.639 $M_J$, 1.100 AU, 0.362, 59.°45, 272.°73) and (3.194 $M_J$, 1.744 AU, 0.249, 5.°34, 199.°70) for the inner and outer planet, respectively. Still, the derived configuration is also unstable and disrupts during about 200,000 yr. Nevertheless, we found that its MEGNO signature is characteristic for a system residing on the border of a stable region rather than a collisional configuration. Thus one may suspect that, in its proximity, a rigorously stable solution can easily be found.

[1] See http://www.hao.ucar.edu/Public/models/pikaia/pikaia.html.

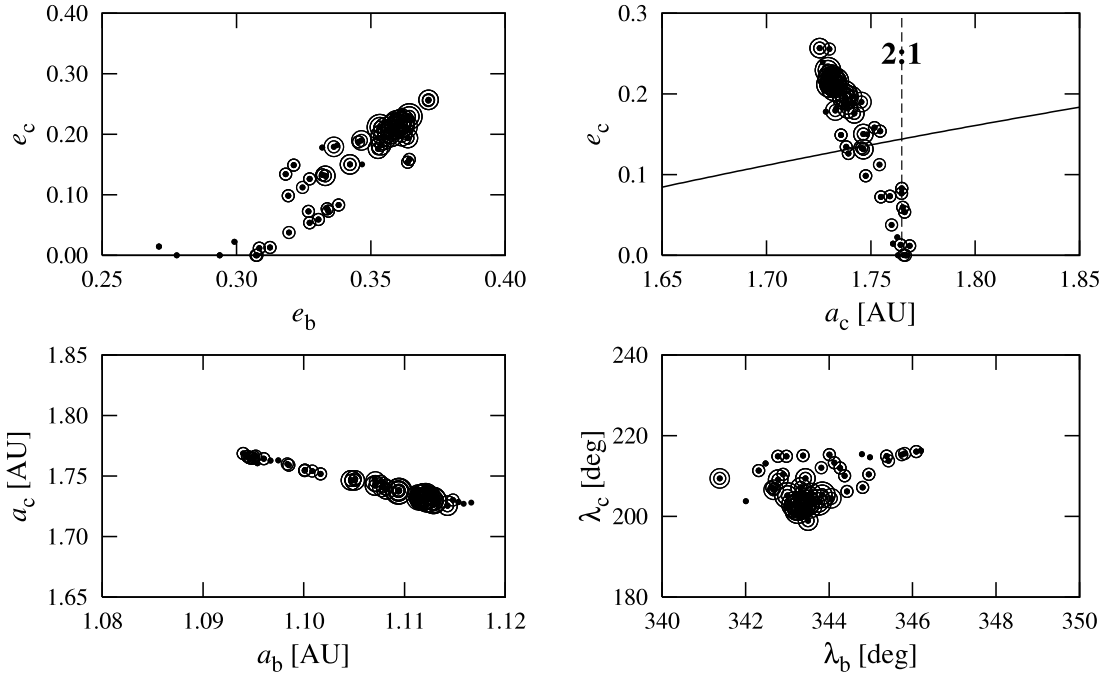


FIG. 1.—Best fits obtained by the GAMP algorithm for the RV data published in Vogt et al. (2005) for HD 128311. In the model, the coplanar system and 2:1 MMR is assumed. Parameters of the fit are projected onto the planes of osculating orbital elements. The smallest filled circles are for the solutions with $(\chi^2_\nu)^{1/2}$ within the formal 3 $\sigma$ confidence interval of the best-fit solution, with $(\chi^2_\nu)^{1/2} < 1.79$. Bigger open circles are for $(\chi^2_\nu)^{1/2} < 1.761$ and $(\chi^2_\nu)^{1/2} < 1.741$ (2 and 1 $\sigma$ confidence intervals of the best-fit solution, respectively). The largest circles are for the solutions with $(\chi^2_\nu)^{1/2} < 1.732$, marginally larger than $(\chi^2_\nu)^{1/2} = 1.731$ of the best-fit initial condition (fit I, Table 1). A curve in the $(a_c, e_c)$ plane denotes the planetary collision line that is determined from the relation $a_b(1 + e_b) = a_c(1 - e_c)$ with $a_b$, $e_b$ fixed at their best-fit values. The nominal position of the 2:1 MMR inferred from the Kepler law is also marked.

In order to deal with the problem of an unstable two-planet Keplerian fit, Vogt et al. (2005) applied a method of fitting that incorporates the mutual interaction between planets (Laughlin & Chambers 2001) and also explicitly involves stability criterion. As such, the authors use the maximal eccentricity attained by the companions during an integration time. They report many stable solutions corresponding to the 2:1 MMR. According to the authors, their best fit yields an rms $\sim$14.7 m s$^{-1}$ and $(\chi^2_\nu)^{1/2} \sim 1$. We could not reproduce that value of $(\chi^2_\nu)^{1/2}$. The quoted $(\chi^2_\nu)^{1/2}$ could be misprinted, or a jitter estimate larger than $\sim$9 m s$^{-1}$ could have been used in the calculations.

For a comparison with that result and as a background for further analysis, we performed the GAMP search for the best-fit solution to the RV data from Vogt et al. (2005), assuming that a 2:1 resonance is indeed present in the coplanar and edge-on systems. We also explored a more general model in which the orbits are mutually inclined, but we did not find substantially better fits.

In Figure 1, the elements of the best-fit solutions from the GAMP runs are shown in a few representative planes of the osculating elements at the date of the first observation, JD 2,450,983.827. In the GAMP code, the MEGNO was evaluated over 1000–5000 orbital periods of the outer planet, which is both efficient enough and makes it possible to withdraw strongly chaotic, unstable solutions. The best-fit initial conditions are marked with symbols of different sizes; larger circles indicate a smaller $(\chi^2_\nu)^{1/2}$ (a better fit). Only *stable* solutions within the 3 $\sigma$ confidence interval of the best-fit solution (given in Table 1) are shown. Overall, the statistics of initial conditions shown in Figure 1 are in accord with the results of Vogt et al. (2005; see their Fig. 12). The permitted *initial* eccentricities of the fits span a skewed and narrow valley in the $(e_b, e_c)$ plane. Let us note that we represent the *N*-body initial conditions in terms of astrocentric, osculating Kepler elements at the epoch of the first observation.

The orbital elements for the outer planet have larger errors than those for the inner one. Both semimajor axes and phases are already very well determined. The parameters of the stable best-fit solution are given in Table 1 (fit I). Note that this strictly regular solution has $(\chi^2_\nu)^{1/2} \simeq 1.731$ and rms $\simeq$15.28 m s$^{-1}$. A very similar value of $(\chi^2_\nu)^{1/2}$ in the *N*-body and Keplerian fits means that the mutual interactions between planetary companions are not evident in the Doppler signal spanning 10 yr. Nevertheless, we stress that the stability constraints are essential for obtaining stable configuration of the *N*-body model.

In Figure 2, we show the stability analysis for the best fit solution corresponding to a 2:1 MMR (fit I given in Table 1). The spectral number, log SN, as well as max $e_{b,c}$, the maximal eccentricities of both planets, and max $\theta$, the maximal $\theta = \varpi_b - \varpi_c$ (where $\varpi_{b,c}$ are the longitudes of pericenters) attained during the integration over $\sim 7 \times 10^4$ orbital periods of the outer body are shown in subsequent panels of Figure 2. It turns out that the best-fit solution lies on the border of an island related to the corotation of apsides ($\theta$, as well as the critical arguments of the 2:1 MMR, is librating about 0° with a large amplitude). The border of the stable resonance zone that is present in the SN-map can also be seen in all other maps, in particular in the max *e* maps. This is a strong argument that the formal stability criterion is in a one-to-one relationship with the behavior of the system. Clearly, the search zone for the best-fit solution should be limited to the resonance island, which constantly changes its shape when we change the orbital parameters. Thanks to the instability penalty in our approach, we have confidence that the obtained solution is indeed optimal [i.e., it minimizes $(\chi^2_\nu)^{1/2}$ and is dynamically stable].

In our next test, we carried out a search for a stable Trojan configuration. Our model was extended to 14 osculating orbital elements, including the inclinations and one nodal longitude as free parameters. Note that due to very similar orbital semimajor axes, the planets are numbered by giving the symbol "b" to the

TABLE 1

Best-fit Two-Planet Initial Conditions for HD 128311 and HD 82943

| | Fit I HD 128311 (2:1 MMR) | | Fit II HD 128311 (1:1 MMR) | | Fit III HD 82943 (2:1 MMR) | | Fit IV HD 82943 (1:1 MMR) | |
|---|---|---|---|---|---|---|---|---|
| Orbital Parameter | b | c | b | c | b | c | b | c |
| $m_2 \sin i$ ($M_J$) | 1.606 | 3.178 | 7.174 | 6.954 | 1.810 | 1.816 | 9.888 | 4.182 |
| $a$ (AU) | 1.112 | 1.732 | 1.737 | 1.796 | 0.744 | 1.192 | 1.187 | 1.201 |
| $e$ | 0.359 | 0.214 | 0.311 | 0.599 | 0.394 | 0.128 | 0.504 | 0.658 |
| $i$ (deg) | 90.00 | 90.00 | 44.22 | 16.96 | 90.00 | 90.00 | 19.23 | 19.57 |
| $\omega$ (deg) | 71.58 | 12.71 | 84.14 | 112.53 | 121.31 | 223.01 | 123.74 | 126.33 |
| $\Omega$ (deg) | 0.0 | 0.0 | 209.79 | 0.0 | 0.0 | 0.0 | 178.52 | 0.0 |
| $M(t_0)$ (deg) | 271.72 | 190.23 | 125.24 | 311.56 | 355.99 | 258.80 | 356.02 | 170.30 |
| $V_0$ (m s$^{-1}$) | 0.970 | | 0.655 | | −0.782 | | −2.877 | |
| $(\chi^2_\nu)^{1/2}$ | 1.731 | | 1.797 | | 1.047 | | 1.221 | |
| rms (m s$^{-1}$) | 15.28 | | 15.49 | | 7.12 | | 8.13 | |

Note.—The best-fit two-planet initial conditions for the HD 128311 (Vogt et al. 2005) and HD 82943 (Mayor et al. 2004) planetary systems found with GAMP (MEGNO was calculated over $\simeq$1000–5000 periods of the more distant companion). Jitter estimates are 9 m s$^{-1}$ for HD 128311 and 5 m s$^{-1}$ for HD 82943. Astrocentric osculating elements are given for the date of the first observation from Vogt et al. (2005) and Mayor et al. (2004), respectively. The masses of the parent stars are 0.84 $M_\odot$ for HD 128311 and 1.15 $M_\odot$ for HD 82943.

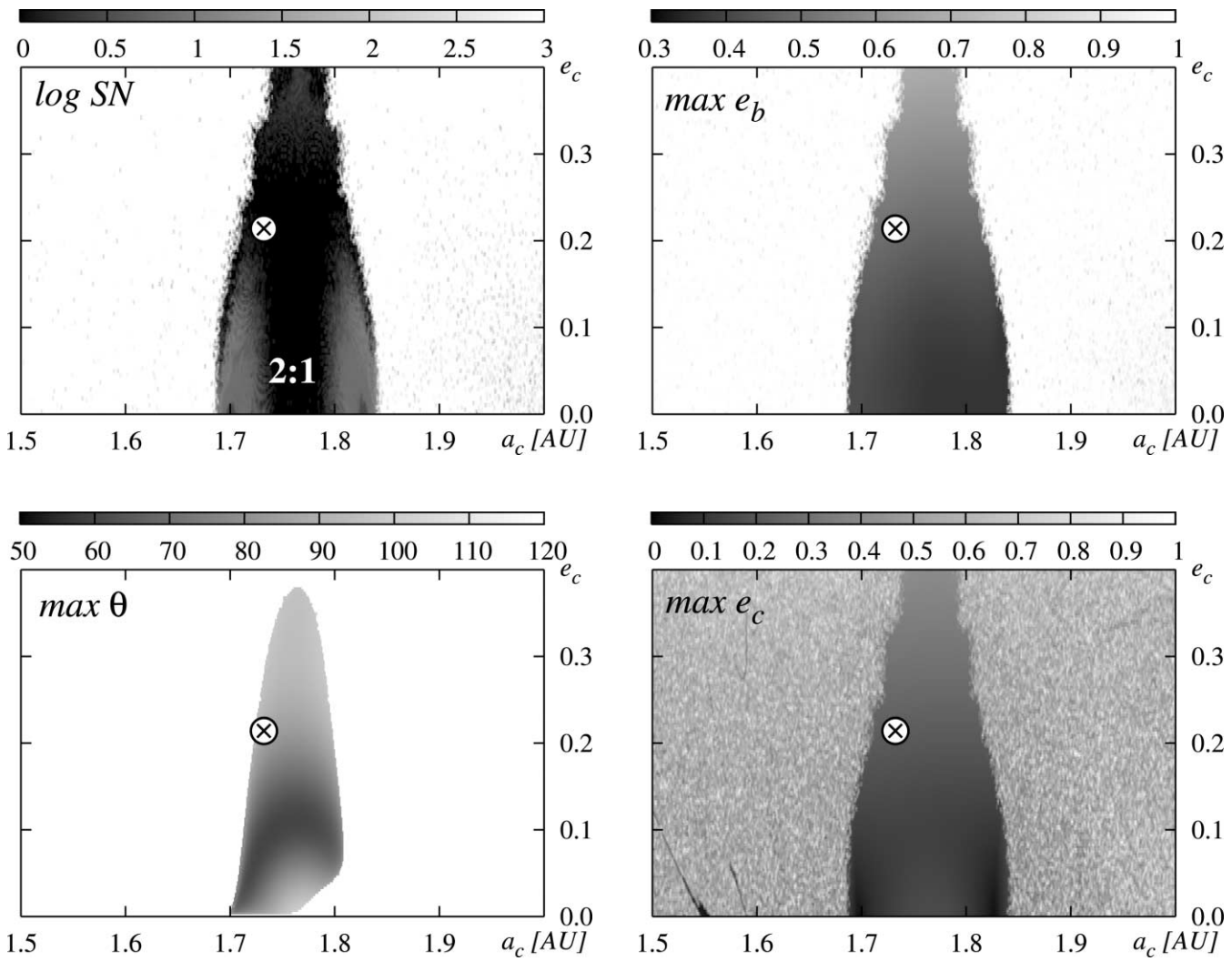


Fig. 2.—Stability maps in the $(a_c, e_c)$ plane in terms of the spectral number, log SN, max $e$, and max $\theta$ for the best-fit solution corresponding to the putative 2:1 MMR for the coplanar HD 128311 system (see Table 1, fit I). Colors used in the log SN map classify the orbits: black indicates quasi-periodic, regular configurations, while white indicates strongly chaotic systems. A circle denotes the best-fit configuration related to fit I. The resolution of the maps is $600 \times 120$ data points. Integrations are for $3 \times 10^4$ periods of the outer planet ($\sim 7 \times 10^4$) yr. [*See the electronic edition of the Journal for a color version of this figure.*]

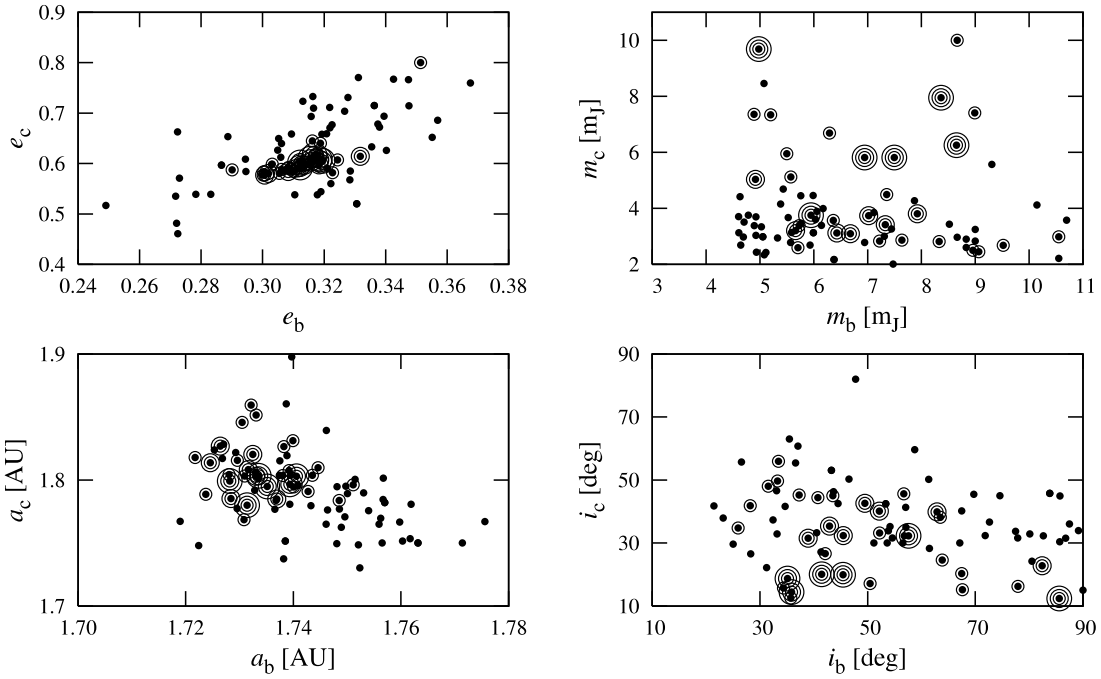


FIG. 3.—Solutions obtained with GAMP for the RV data from Vogt et al. (2005) for HD 128311. In the model, an inclined system and a 1:1 MMR is assumed. Orbital parameters are projected onto the planes of osculating elements. The smallest filled circles are for solutions with $(\chi^2_\nu)^{1/2}$ within the formal 3 $\sigma$ confidence interval of the best fit (fit II in Table 1) with $(\chi^2_\nu)^{1/2} < 1.9$ and the rms about 17 m s$^{-1}$. The bigger open circles are for $(\chi^2_\nu)^{1/2} < 1.825$ and $(\chi^2_\nu)^{1/2} < 1.81$ (2 and 1 $\sigma$ confidence intervals, respectively). The largest circles are for the solutions with $(\chi^2_\nu)^{1/2} < 1.799$, marginally larger than $(\chi^2_\nu)^{1/2} = 1.797$ of the best fit II. Compare the formal 3 $\sigma$ range for the solutions shown in the ($a_b$, $a_c$) plane with the width of the 1:1 MMR for the best-fit solution (Fig. 6, *bottom row*).

planet that has a smaller initial eccentricity. As one can see in Figure 3, a well-defined minimum of $(\chi^2_\nu)^{1/2}$ is present in the $(a_b, a_c)$ and $(e_b, e_c)$ planes. The best-fit inclinations are not very well constrained, nevertheless their concentration is quite evident, in spite of the moderate time span of the observations.

The osculating elements of the best-fit solution are given in Table 1 (fit II). Its $(\chi^2_\nu)^{1/2} \simeq 1.797$ and rms $\simeq$15.48 m s$^{-1}$ are very close to those of the 2:1 MMR configuration. The synthetic RV signals of both solutions are shown in Figure 4. They can barely be distinguished from one another. We also computed the Lomb-Scargle periodograms of both synthetic signals, and we plotted them together with the periodogram of the data set in Figure 5. It shows that periodograms of the 2:1 and 1:1 configurations almost perfectly match. It would be very difficult to distinguish between the configurations by looking only at the periodograms.

The best-fit Trojan configuration resides in a wide, stable zone in the plane of the eccentricities that extends up to 1 for both of these elements (see Fig. 6). The resonance area in the $(a_c, e_c)$ plane covers about 0.2 AU. This width is even larger than for the 2:1 MMR configuration (see Fig. 2). Obviously, the stable 1:1 MMR is possible due to the corotation of the apsides seen in the max $\theta$ maps ($\theta$ librates about 180°).

Our choice of the stability criterion enables us to obtain very sharp borders of the resonance area. If this criterion were violated, the system would quickly disrupt (because both $e$'s go to 1). In Figure 7, we show the stability maps for a solution that has an rms of about 15.7 m s$^{-1}$ (slightly more than the best one; see the caption to Fig. 7) and corresponds to much smaller masses (both initial inclinations are about 45°). Essentially, the dynamical features of the system do not change, but the width of the resonance zone shrinks substantially. This is also an argument that an appropriate stability criterion has to be an integral part of the

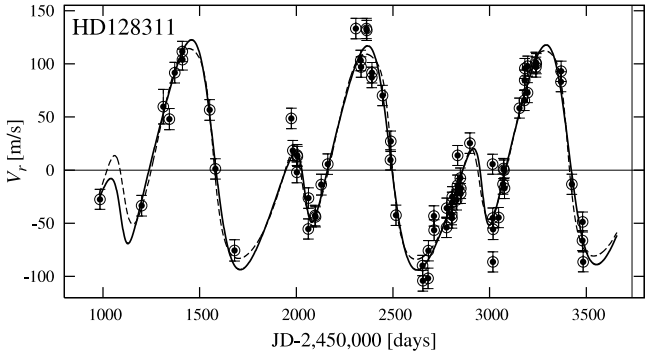


FIG. 4.—Synthetic RV curves for the best-fit solutions corresponding to the 2:1 and 1:1 MMRs in the HD 128311 planetary system (see also Table 1, Fits I and II). The thick line is for the 1:1 MMR and the dashed line is for the 2:1 MMR. Both curves give an rms of $\simeq$15 m s$^{-1}$. The error bars include the stellar jitter of 9 m s$^{-1}$.

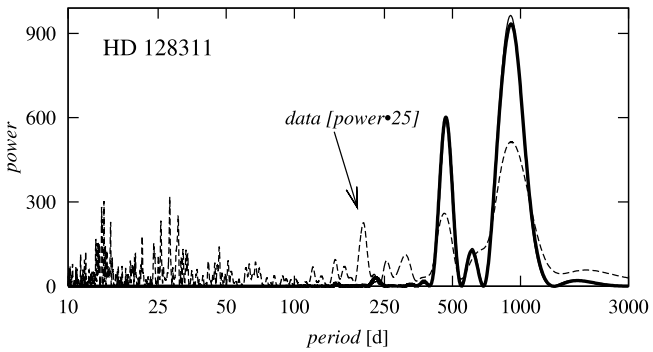


FIG. 5.—Lomb-Scargle periodogram for the best-fit solutions found for the HD 128311 system (fits I and II in Table 1). The thick line is for the synthetic RV corresponding to the 2:1 MMR. The thin line is for the RV curve of the 1:1 MMR solution. The dashed line is for the measurements.

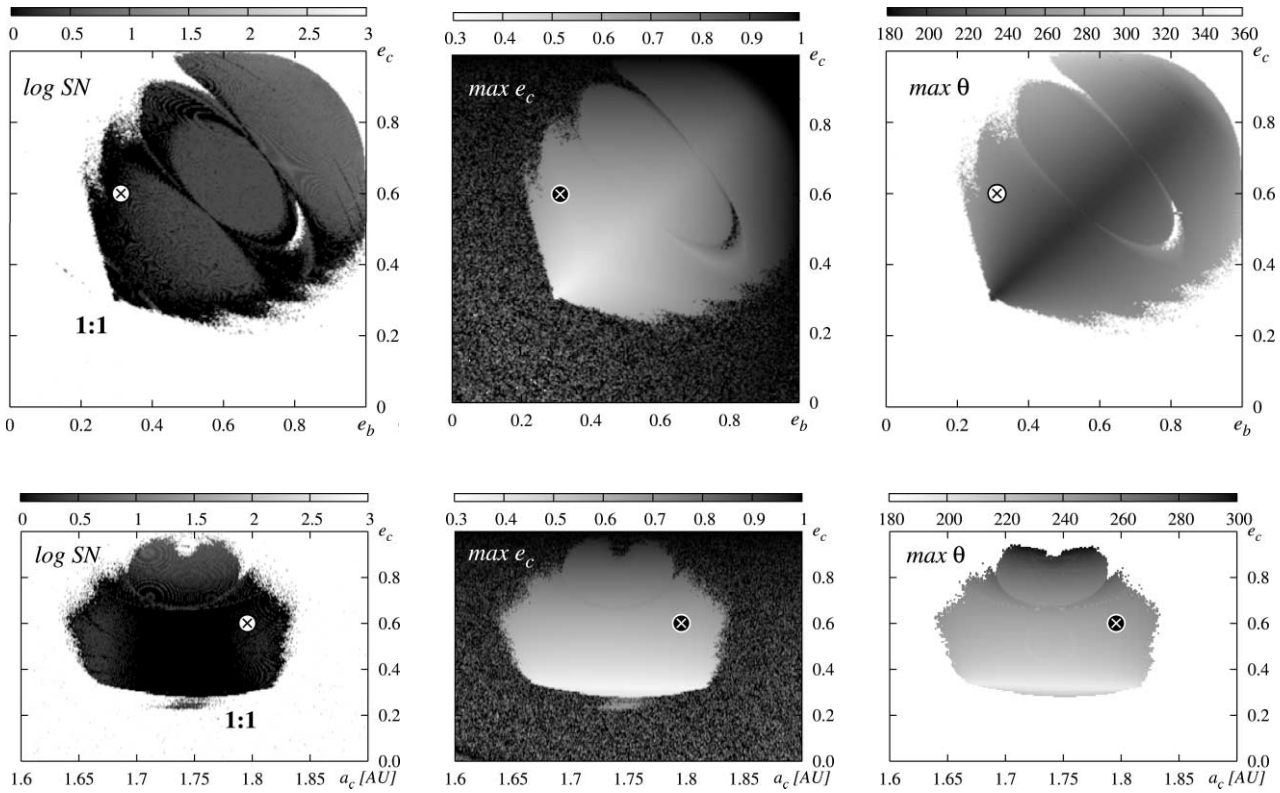


FIG. 6.— Stability maps in the ($e_b$, $e_c$) (*top row*; the resolution is $250 \times 250$ data points) and ($a_c$, $e_c$) planes (*bottom row*; the resolution is $480 \times 200$ data points) for HD 128311 (fit II). The left column is for the spectral number, log SN. Colors used in the log SN map classify the orbits; black indicates quasi-periodic, regular configurations while white indicates strongly chaotic systems. The maps marked with max $e_c$ and max $\theta$ are respectively for the maximal eccentricity and the maximum of $\theta = \varpi_b - \varpi_c$ attained during the integration of the system. A circle marks the parameters of the best-fit solution. The integration was conducted for $\sim 6 \times 10^4$ orbital periods of the planets. [*See the electronic edition of the Journal for a color version of this figure*.]

fitting tool. Due to the extremely nonlinear nature of the system, even a small change of its initial elements can lead to a significant change in the shape of the resonance zone. Simultaneously, max $e$ becomes very "flat" in the regions of large $e$, so max $e$ would not be a convenient stability indicator in a GAMP-like code. Another argument is that the variable rate of the chaotic diffusion that leads to the changes of the eccentricity can sometimes be too small to detect a collision or a qualitative change of the configuration over relatively short integrations, which, for efficiency reasons, have to be limited to the timescale of the MMRs. One might think that (again, mainly for efficiency reasons) max $\theta$ would be a better choice than both max $e$ and MEGNO as a stability criterion. However, that test may also fail, since in the resonance zone, the critical angle $\theta$ may librate about different centers (usually, about $0^\circ$ or $180^\circ$), but it can circulate in some marginally unstable regions as well (see the Appendix for details).

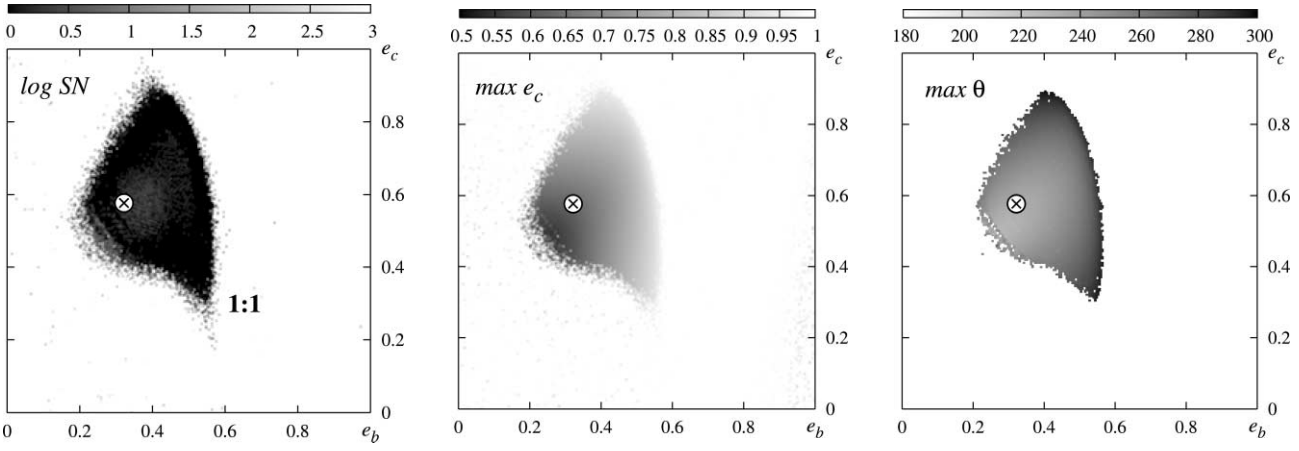


FIG. 7.— Stability maps in the ($e_b$, $e_c$) plane (the resolution is $250 \times 250$ data points) for the fit of the 1:1 MMR in the HD 128311 system having a slightly larger rms than the best-fit solution (fit II in Table 1), $\simeq 15.7$ m s$^{-1}$ and $(\chi^2_\nu)^{1/2} = 1.82$. The osculating elements at the date of the first observation are ($m$ [$M_J$], $a$ [AU], $e$, $i$ [deg], $\Omega$ [deg], $\omega$ [deg], and $M$ [deg]): (7.22, 1.730, 0.323, 43.52, 220.38, 80.18, and 129.99) for the planet b and (2.83, 1.816, 0.582, 45.00, 0.00, 113.43, and 312.87) for the planet c; $V_0 = -0.078$ m s$^{-1}$. The left column is for the spectral number, log SN. Colors used in the log SN map classify the orbits; black indicates quasi-periodic, regular configurations while white indicates strongly chaotic systems. The maps marked by max $e_c$ and max $\theta$ are respectively for the maximal eccentricity of the outermost planet and the maximum of $\theta = \varpi_b - \varpi_c$ attained during the integration of the system. A circle marks the parameters of the best-fit solution. The integration was conducted for $\sim 6 \times 10^4$ orbital periods of the planets. [*See the electronic edition of the Journal for a color version of this figure*.]

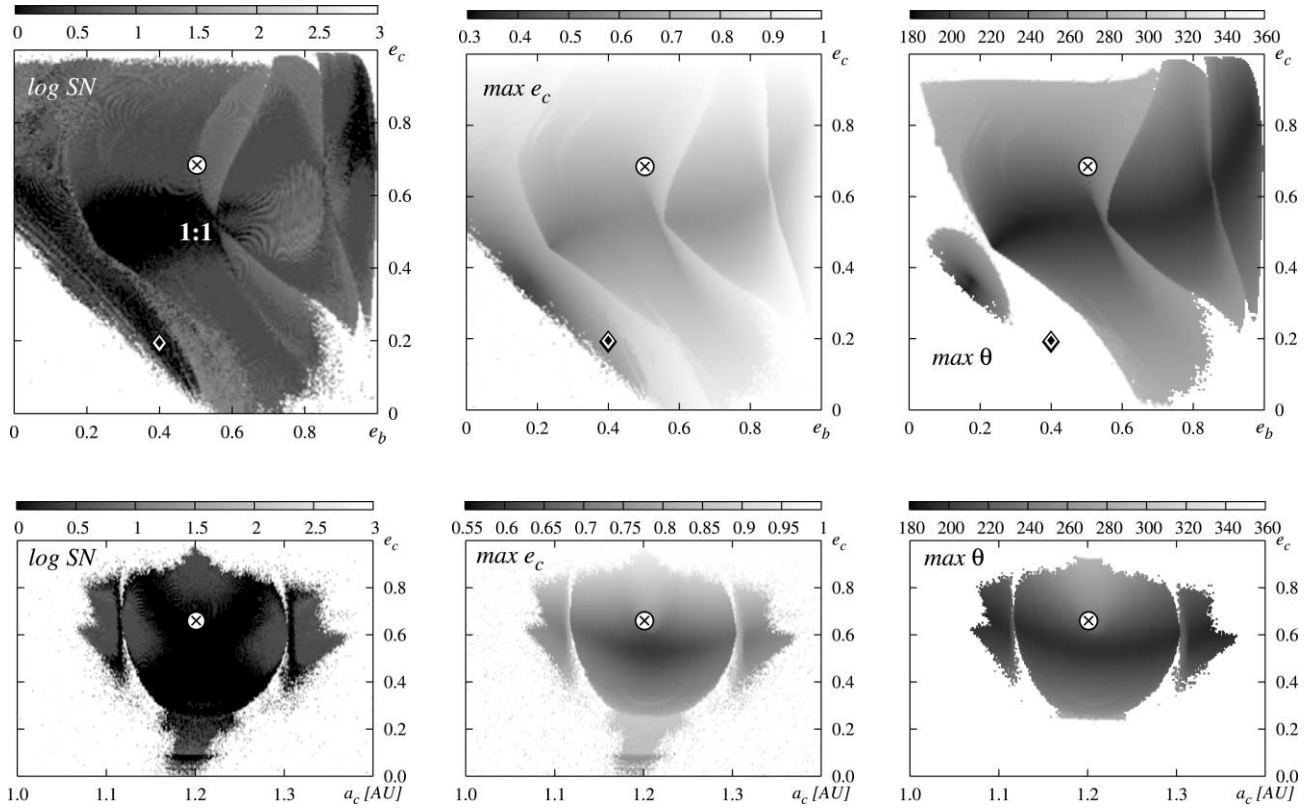


FIG. 8.—Stability maps in the ($e_b$, $e_c$) (*top row*; the resolution is $250 \times 250$ data points) and ($a_c$, $e_c$) planes (*bottom row*; the resolution is $400 \times 200$ data points) for HD 82943 (fit IV, see Table 1). The left column is for the spectral number, log SN. Colors used in the log SN map classify the orbits; black indicates quasi-periodic, regular configurations while white indicates strongly chaotic systems. The maps marked by max $e_c$ and max $\theta$ are respectively for the maximal eccentricity and the maximum of $\theta = \varpi_b - \varpi_c$ attained during the integration of the system. A circle marks the parameters of the best-fit solution corresponding to the 1:1 MMR in the HD 82943 system (fit IV, Table 1). The integration was conducted for $\sim 6 \times 10^4$ orbital periods of the planets. The diamond at ($e_b = 0.4, e_c = 0.2$) is for the initial condition in a discussion of the proper choice of the stability indicator in the GAMP-like code (see the Appendix). [*See the electronic edition of the Journal for a color version of this figure.*]

## 4. HD 82943

The HD 82943 planetary system (Mayor et al. 2004) has drawn the attention of many researchers (e.g., Goździewski & Maciejewski 2001; Ji et al. 2003; Ferraz-Mello et al. 2005; Lee et al. 2006). The two-planet Keplerian solutions produced by the discovery team correspond to catastrophically unstable configurations (Goździewski & Maciejewski 2001; Ferraz-Mello et al. 2005; Lee et al. 2006). The discovery team did not publish the observations of HD 82943 in source form. The method of dealing with the problem of unavailable RV data relies on digitizing the published figures depicting the measurements. This somewhat unusual approach has already become an accepted procedure (e.g., Goździewski & Maciejewski 2001; Goździewski & Konacki 2004; Ferraz-Mello et al. 2005; Lee et al. 2006).

First, we digitized 142 data points from the figures of Mayor et al. (2004). They differ slightly from the real observations. In particular, it is difficult to recover the exact moments of the observations (Ferraz-Mello et al. 2005), but such digitized measurements still properly describe the overall shape of the observed RV curve and its characteristic features. We also graphically derived the measurement errors and rescaled them by adding, in quadrature, the stellar jitter which we estimated as $\sim 5$ m s$^{-1}$ on the basis of Wright (2005).

Having such "measurements," we recovered the best-fit two-planet Keplerian solutions published by the discovery team (Mayor et al. 2004). The only problem seems to be a slightly larger value of the rms of $\simeq 7.1$ m s$^{-1}$ (compared to 6.8 m s$^{-1}$ quoted in the original work). Using the digitized RV measurements, Ferraz-Mello et al. (2005) showed that stable 2:1 MMR configurations are possible. Their orbital parameters of coplanar, edge-on systems are similar to those we found with GAMP (fit III in Table 1). We note that these authors looked for the best-fit solutions by minimizing the rms rather than $(\chi^2_\nu)^{1/2}$, and they did not increase the internal errors by jitter. Also, the discovery team did not account for the jitter in their solutions.

We extended the search for the best-fit solution, assuming that a 1:1 MMR can be present in the HD 82943 system. As in the previous case, we did not find any stable, strictly coplanar, edge-on configuration of this type. However, using the generalized model in which masses, inclinations, and one nodal longitude are free parameters, we found many stable solutions. Their quality is not as good as for the 2:1 MMR; the best 1:1 MMR fit has $(\chi^2_\nu)^{1/2} \simeq 1.2$, and the rms is $\simeq 8.1$ m s$^{-1}$, which is about 1 m s$^{-1}$ worse than for our best 2:1 MMR solution. Still, the 1:1 MMR solution may be plausible (note that we use digitized "observations"). Also, since the mass of the parent star cannot be determined precisely (Ferraz-Mello et al. 2005), when new measurements are available, the best-fit parameters and their $(\chi^2_\nu)^{1/2}$ may change. We demonstrate this in the next section.

The best-fit 1:1 MMR configuration (fit IV in Table 1) is characterized by initially large mutual orbital inclination because, although the inclinations for both planets are almost the same, the nodal longitude is about 180° (and the apsidal lines are antialigned). The orbital evolution leads to quite large variations of the orbital inclinations (a few tens of degrees). The stability maps shown in Figure 8 reveal that, apparently, such a system would be locked in an extremely large zone of stable motions that

TABLE 2
BEST-FIT TWO-PLANET INITIAL CONDITIONS FOR HD 82943

| | FIT V (STABLE) HD 82943 (2:1 MMR) | | FIT VI (STABLE) HD 82943 (1:1 MMR) | | FIT VII (UNSTABLE) HD 82943 (2:1 MMR) | | FIT VIII (STABLE) HD 82943 (THREE-PLANET) | | |
|---|---|---|---|---|---|---|---|---|---|
| ORBITAL PARAMETER | b | c | b | c | b | c | b | c | d |
| $m_2 \sin i$ ($M_J$) | 1.461 | 1.728 | 2.043 | 3.932 | 17.16 | 1.761 | 1.679 | 1.867 | 0.487 |
| $a$ (AU) | 0.748 | 1.186 | 1.208 | 1.180 | 0.751 | 1.240 | 0.751 | 1.197 | 2.125 |
| $e$ | 0.448 | 0.268 | 0.640 | 0.500 | 0.380 | 0.001 | 0.386 | 0.110 | 0.018 |
| $i$ (deg) | 90.00 | 90.00 | 49.35 | 56.56 | 6.260 | 87.85 | 90.0 | 90.0 | 90.0 |
| $\omega$ (deg) | 126.82 | 138.35 | 133.92 | 127.88 | 119.84 | 187.81 | 118.08 | 144.47 | 114.61 |
| $\Omega$ (deg) | 0.0 | 0.0 | 145.71 | 0.0 | 346.23 | 0.0 | 0.0 | 0.0 | 0.0 |
| $M(t_0)$ (deg) | 359.23 | 336.85 | 186.39 | 353.84 | 0.00 | 286.03 | 2.65 | 345.24 | 79.76 |
| $V_0$ (m s$^{-1}$) | 13.66 | | 12.41 | | 15.42 | | 14.60 | | |
| $V_1$ (m s$^{-1}$) | −7.72 | | −6.86 | | −4.96 | | −0.73 | | |
| $(\chi^2_\nu)^{1/2}$ | 1.39 | | 1.45 | | 1.32 | | 1.27 | | |
| rms (m s$^{-1}$) | 7.98 | | 8.40 | | 7.58 | | 7.36 | | |

NOTE.—Best-fit two-planet initial conditions for the HD 82943 planetary system on the basis of a data set used by Lee et al. (2006). The stable fits are found with GAMP (MEGNO was calculated over ≃1000–5000 periods of the more distant companion). Jitter estimate is 4.2 m s$^{-1}$. Astrocentric osculating elements are given for the date of the first observation from Mayor et al. (2004). The mass of the parent star is 1.15 $M_\odot$. CORALIE RV data are shifted by 8128.598 m s$^{-1}$.

extends up to $e_{b,c} \sim 1$. This means that the eccentricities could reach extremely large values, but the system would still be stable. The width of the resonance with respect to $a_c$ is also relatively large, about 0.2 AU. A zone of strictly periodic motions can be seen in the map for max $\theta$, close to its diagonal.

### 4.1. *Fits for HD 82943 Revisited*

We extended the analysis of HD 82943 after gaining access to the same data set used by Lee et al. (2006; also Lee 2005, private communication). These authors also used the "digitized" measurements from Mayor et al. (2004) but added new observations obtained with the Keck HIRES (High Resolution Echelle Spectrometer). These new, very accurate data fill in some gaps in the CORALIE measurements as well as significantly increase the time span of the observations. For consistency with Lee et al. (2006), we adopted the jitter estimate of 4.2 m s$^{-1}$.

The results of fitting two-planet Keplerian models and the analysis of their stability by Lee et al. (2006) strongly confirm the possibility of a stable 2:1 MMR in the HD 82943 system. Still, new questions may be asked. The best fit of the 2:1 MMR configuration yields an rms ∼8 m s$^{-1}$, which is unexpectedly larger by 1 m s$^{-1}$ than that quoted for the CORALIE data by the discovery team, Mayor et al. (2004) and by Ferraz-Mello et al. (2005), as well as in this work.

For the updated data set, we recovered all the best-fit Keplerian solutions quoted by Lee et al. (2006) using our GA/simplex code.

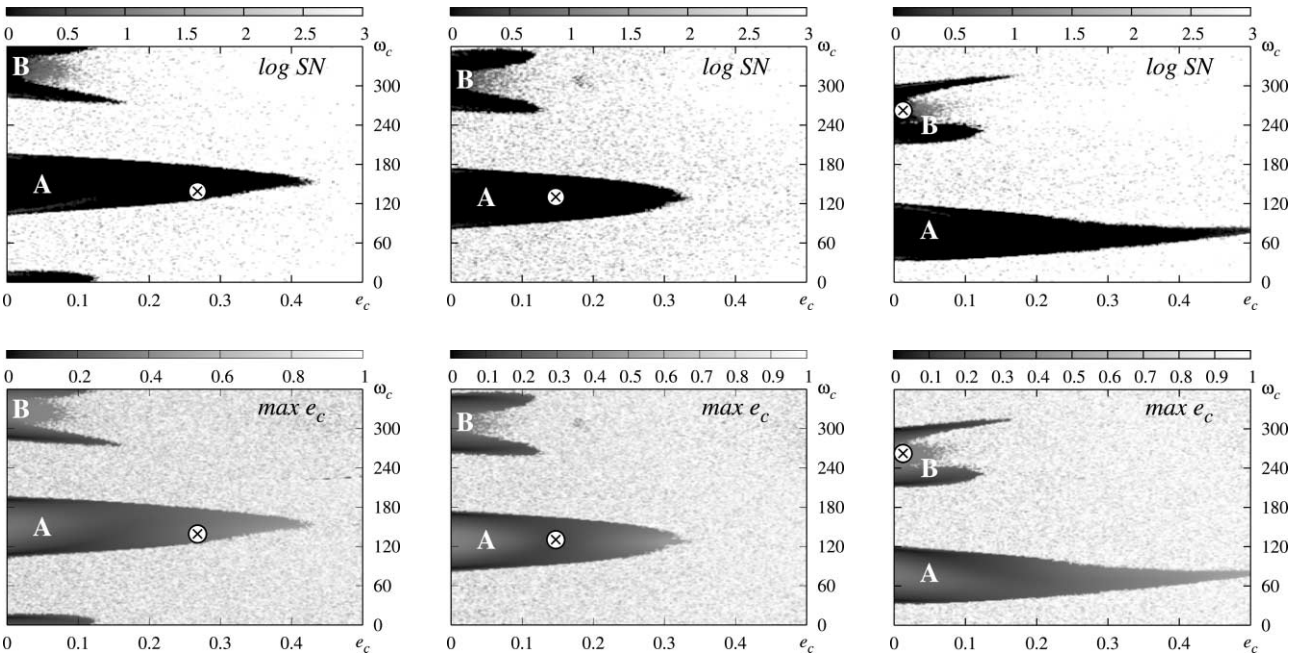


FIG. 9.—Stability maps in the ($e_c$, $\omega_c$) plane of the HD 82943 system (the resolution is 240 × 240 data points) for the two-planet edge-on best-fit solutions related to the 2:1 MMR in the HD 82943 system. The left column is for the best stable fit V (Table 2). The right column is for the alternative, marginally worse solution with the following astrocentric elements ($m_p \sin i$, $a$, $e$, $\omega$, $M$) at the epoch of the first observation: (1.781 $m_J$, 0.748 AU, 0.399, 118°.273, 0°.000) and (1.773 $M_J$, 1.194 AU, 0.012, 261°.882, 221°.483) for the inner and outer planet, respectively; an rms of this fit is ∼8.1 m s$^{-1}$. The middle column is for a two-planet Keplerian fit II of Lee et al. (2006). The bottom row is for the spectral number, log SN. The colors used in the log SN map classify the orbits; black indicates quasi-periodic regular configurations while white indicates strongly chaotic ones. The maps in the top row marked with max $e_c$ are for the maximal eccentricity of the outermost planet attained during the integration of the system. The circle marks the parameters of the best-fit solutions. The integrations were conducted for ∼4 × 10$^4$ orbital periods of the outermost planet. [*See the electronic edition of the Journal for a color version of this figure*.]

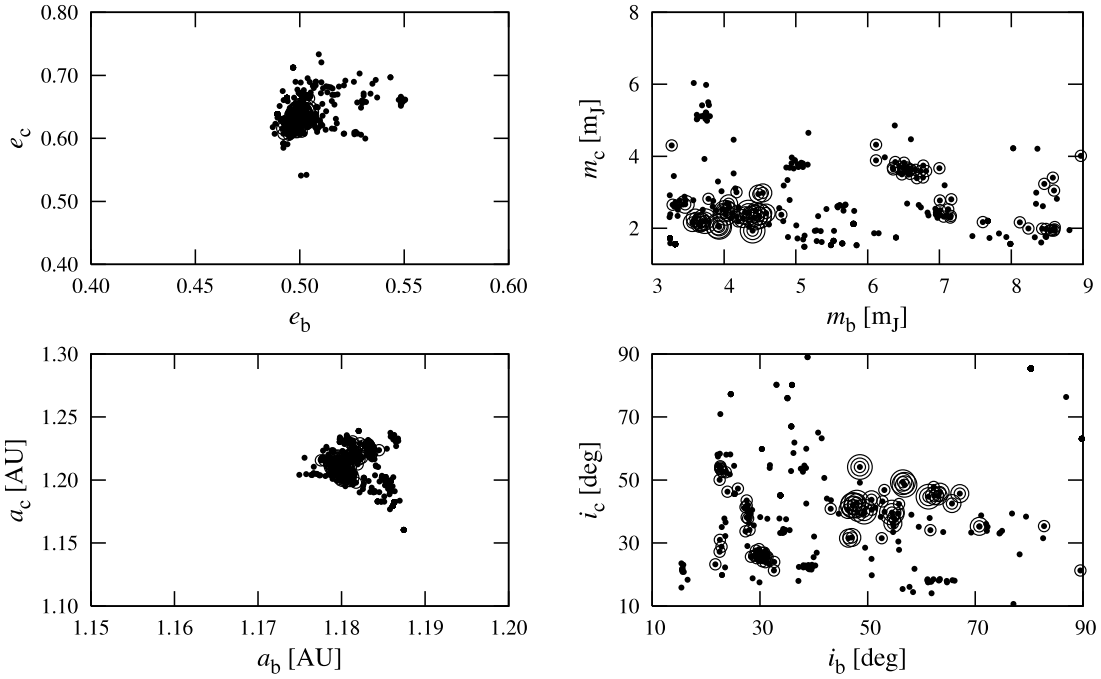


FIG. 10.— Solutions obtained with GAMP for the RV data from Lee et al. (2006) for HD 82943. In the model, mutually inclined orbits and the presence of the 1:1 MMR are assumed. Orbital parameters are projected onto the planes of osculating elements. The smallest filled circles are for solutions with $(\chi^2_\nu)^{1/2}$ within the formal 3 $\sigma$ confidence interval of the best fit (fit VI in Table 2); $(\chi^2_\nu)^{1/2} < 1.55$ and the rms is about 9 m s$^{-1}$. Bigger open circles are for $(\chi^2_\nu)^{1/2} < 1.46$ and $(\chi^2_\nu)^{1/2} < 1.45$ (2 and 1 $\sigma$ confidence intervals, respectively). The largest circles are for the solutions with $(\chi^2_\nu)^{1/2} < 1.449$, marginally larger than $(\chi^2_\nu)^{1/2} = 1.447$ of the best fit VI given in Table 2.

Some of them appear to be formally chaotic or strongly unstable. Thus, we searched for a stable *N*-body solution using GAMP, assuming that the velocity offsets for the CORALIE and Keck/HIRES data are independent. The best-fit, *rigorously stable* solution corresponding to the 2:1 resonance of an edge-on system is given in Table 2 (fit V). Its quality is not very different from the best solutions found by Lee et al. (2006), but the initial eccentricities are significantly different. Our fit V is most similar to the two-planet Keplerian fit II of Lee et al. (2006). We also found other solutions that are similar to their fits III and IV with respect to small initial $e_c$.

According to the results of Ferraz-Mello et al. (2005) and Lee et al. (2006), $e_c$ and $\omega_c$ are the less constrained parameters of the Kepler fits to the RV data of HD 82943. Thus we computed dynamical maps for the relevant solutions (see Fig. 9 and its caption) as well as for fit II of Lee et al. (2006). These maps reveal two narrow zones of stability in which the best-fit solutions reside. All acceptable (stable) 2:1 MMR fits of HD 82943 likely belong to

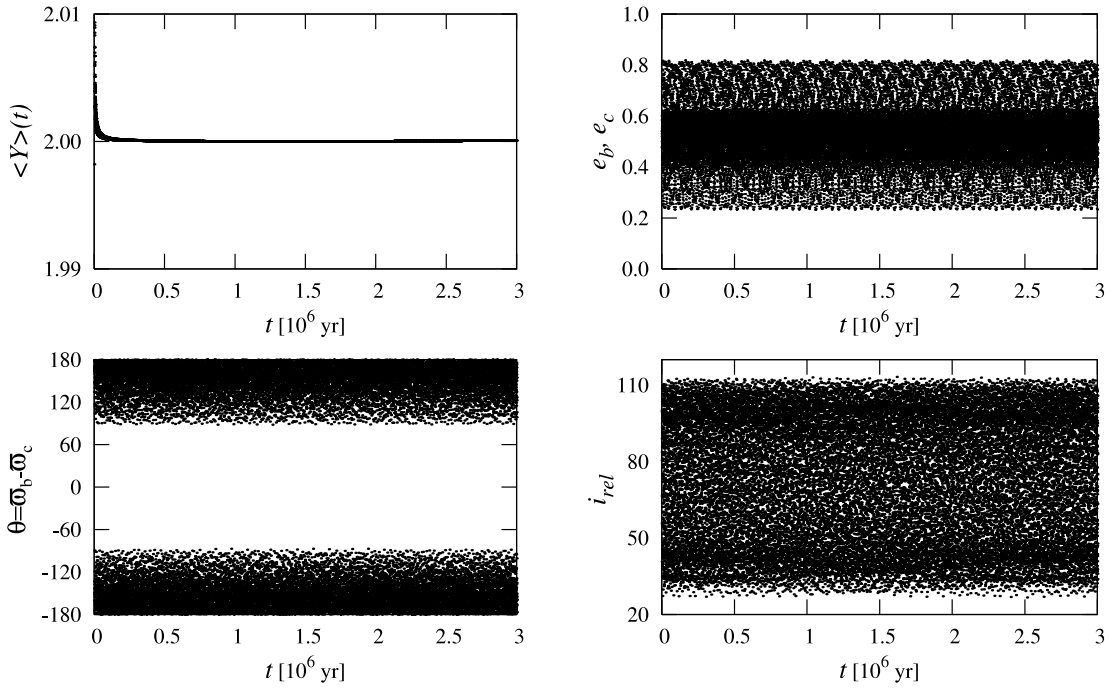


FIG. 11.— Evolution of MEGNO and orbital elements of the configuration described by fit VI in Table 2. A perfect convergence of MEGNO over ~3 Myr indicates a rigorously stable solution. Subsequent panels are for the eccentricities, the critical argument of secular resonance $\theta$, and the relative inclination of orbits, $i_{\rm rel}$.

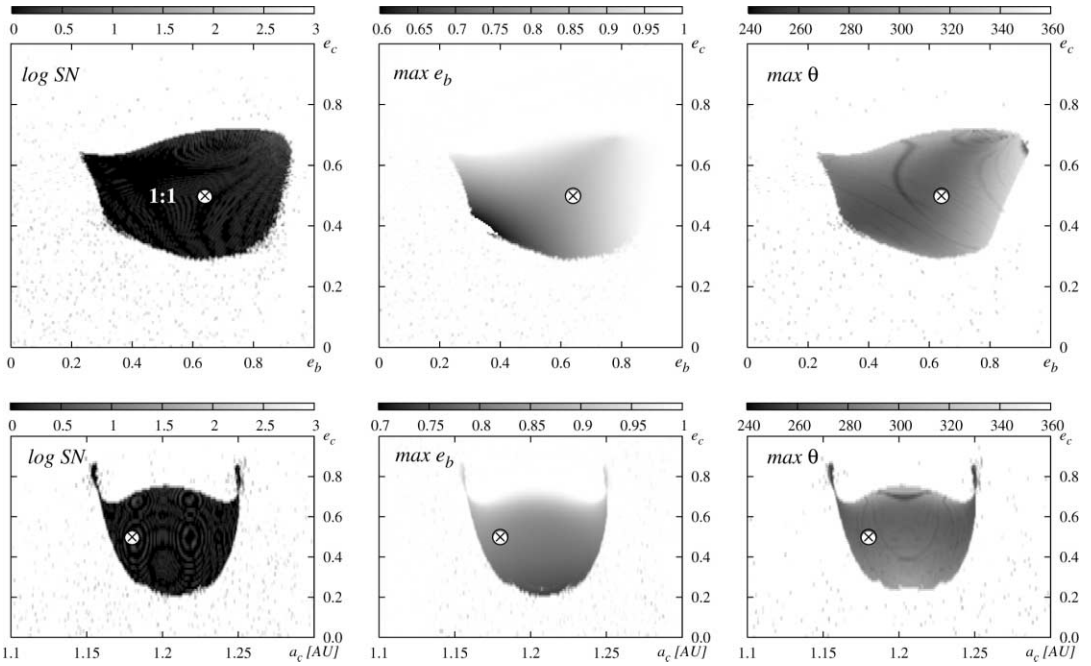


FIG. 12.— Stability maps in the $(e_b, e_c)$ (*top row*, the resolution is $250 \times 240$ data points) and $(a_c, e_c)$ planes (*bottom row*, the resolution is $300 \times 100$ data points) for HD 82943 (fit VI, see Table 2). The left column is for the spectral number, log SN. Colors used in the log SN map classify the orbits: black indicates quasi-periodic, regular configurations while white indicates strongly chaotic systems. The maps marked by max $e_c$ and max $\theta$ are respectively for the maximal eccentricity and the maximum of $\theta = \varpi_b - \varpi_c$ attained during the integration of the system. A circle marks the parameters of the best-fit solution corresponding to the 1:1 MMR in the HD 82943 system (fit VI, Table 2). The integration was conducted for $\sim 3 \times 10^4$ orbital periods of the planets. [*See the electronic edition of the Journal for a color version of this figure.*]

these two distinct islands. We label them A and B in Figure 9. Note that the positions and shape of the resonance areas are significantly altered when the fit parameters are adjusted. Inside the resonance zone A, the amplitudes of the critical angles may vary in wide ranges. Lee et al. (2006) found that their fit II has very small amplitudes of the critical angles of the 2:1 MMR, $\sim 10^\circ$. Our best *N*-body fit V yields much larger amplitudes, $\sim 40^\circ$. The large amplitudes of the critical angles are also reported by Ferraz-Mello et al. (2005). The resonance island A is characterized by the corotation of apsidal lines. We found that in this zone, max $\theta$ may be very close to the libration center $0^\circ$. For instance, for the dynamical map of fit V, at $(e_c \sim 0.116, \omega_c \sim 127.^\circ 7)$ the variations of max $\theta < 2^\circ$, indicating a strictly periodic solution. In the second island labeled B in Figure 9, max $\theta$ also librates about $0^\circ$, but with large amplitudes.

We can speak about dynamical similarity of the best-fit solutions found so far, having in mind their position in the two resonance zones. The results of the dynamical analysis done by Lee et al. (2006) and in this paper favor the 2:1 MMR fits located in the island A (about $\omega_c \sim 120^\circ$). This zone is extended with respect to the not well-constrained $e_c$, and very small amplitudes of the 2:1 MMR critical angles are possible.

We also found many stable, mutually inclined configurations using the orbital inclinations and one nodal argument as free parameters. Still, all these fits have the rms $\sim 8$ m s$^{-1}$. By releasing the stability requirements in the GAMP code, one finds the best two-planet fit yielding the rms $\sim 7.5$ m s$^{-1}$ (fit VII in Table 2). However, this configuration disrupts in a few hundred years. Curiously, such a solution involves a brown dwarf and a Jovian planet on inclined orbits (mutual inclination of $\sim 80^\circ$).

In fact, our main goal was to perform a possibly extensive search for 1:1 configurations. The statistics of stable solutions gathered in this search are illustrated in Figure 10, in a similar manner as for the HD 128311 system. Qualitatively, the solutions do not differ from the ones we found using the CORALIE data only. The semimajor axes and the eccentricities are very well constrained. The initial inclinations and masses are also bounded to two well-determined local minima of $(\chi^2_\nu)^{1/2}$. The best-fit solution is given in Table 2 (fit VI). Its rms $\sim 8.4$ m s$^{-1}$ is even closer to that of the 2:1 MMR best fit than in the case of the CORALIE data alone. Its MEGNO signature, which indicates a perfectly stable, quasi-periodic configuration, and the evolution of orbital elements during 3 Myr are shown in Figure 11. The relevant dynamical maps of the best fit in the $(e_b, e_c)$ and $(a_c, e_c)$ planes are shown in Figure 12. We also compared periodograms (Fig. 13) of the synthetic curves for the 2:1 MMR, 1:1 MMR, and the measurements (shown in Fig. 14). In this case as well, the periodograms for the 2:1 and 1:1 MMR perfectly match each other.

### 4.2. *The Third Planet in HD 82943?*

The solutions described so far do not explain the curious rms excess that is present in the extended data set. It seems unlikely that the problem is caused by some inconsistency of the measurements

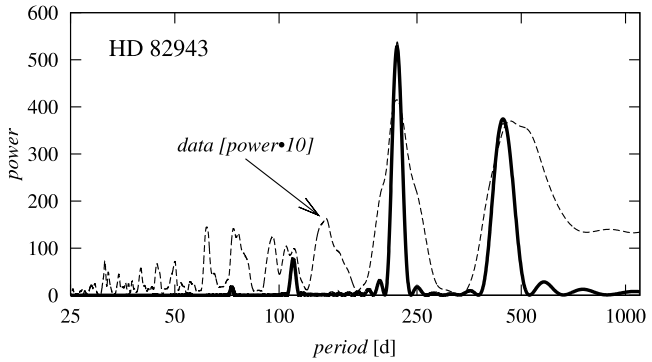


FIG. 13.— Lomb-Scargle periodogram for the best-fit solutions (fits V and VI, Table 2) found for the HD 82943 system. The thick line is for the synthetic RV corresponding to the 2:1 MMR. The thin line is for the RV curve of the 1:1 MMR solution. The dashed line is for the measurements from Lee et al. (2006).

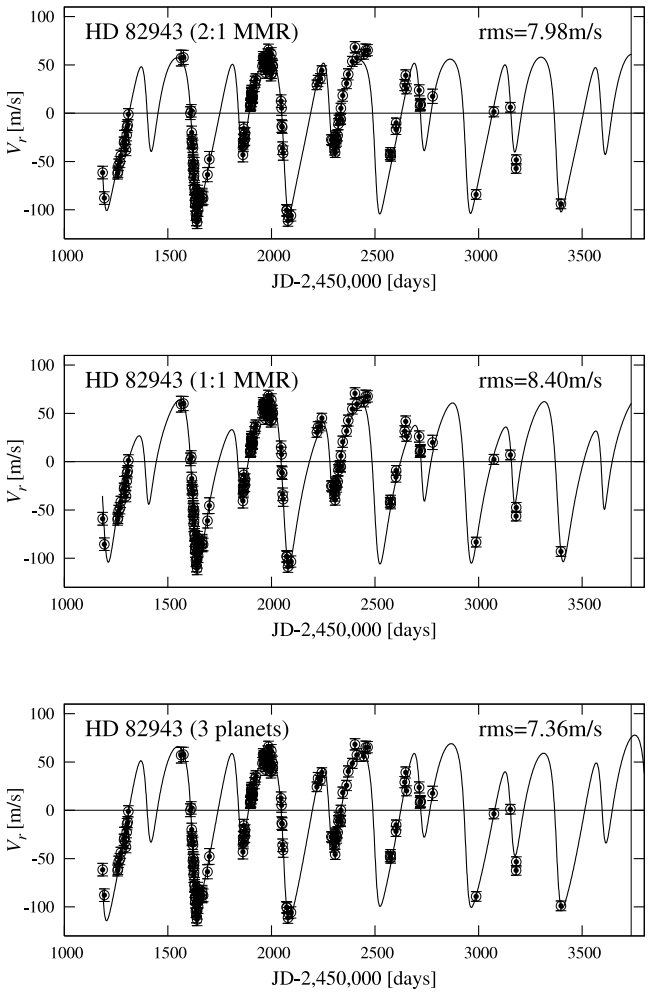


FIG. 14.—Synthetic RV curves for the HD 82943 system. The top plot is for a stable (*N*-body) solution corresponding to a 2:1 MMR (fit V). The middle plot is for the 1:1 MMR solution (fit VI). The bottom plot is for stable Newtonian, three-planet best-fit solution (fit VIII). The open circles are for the RV measurements from Lee et al. (2006). The error bars include stellar jitter of 4.2 m s$^{-1}$.

from the two spectrographs. Another possible explanation is that there is a new, unknown object in the system. That possibility is suggested by Lee et al. (2006). Looking at their Figure 4, which shows the residual signal to the two-planet solutions, we can see a quasi-sinusoidal modulation with a period of about 1000 days. Yet, the jitter estimates of HD 82943 are uncertain by 50% (Lee et al. 2006). Thus, by adopting values as high as 6–7 m s$^{-1}$, one would obtain $(\chi^2_\nu)^{1/2} \sim 1$, and the larger rms would not necessarily be unreasonable. Still, the hypothesis about the third planet is a very attractive explanation of the rms excess. Below, we try to find out whether such a configuration would be consistent with a stable dynamics.

First, we searched for three-planet solutions using the hybrid Kepler code and "blindly" assuming the same bounds of the orbital periods of 10–1200 days and eccentricities of 0–0.8 for every planet. The use of the multiplanet Keplerian model enables us to quickly localize regions of orbital parameters in which potentially stable *N*-body fits can be found. The code was restarted thousands of times. In this search, the algorithm converged to a few distinct local minima yielding similar rms and $(\chi^2_\nu)^{1/2}$.

Remarkably, two of the Keplerian best fits, yielding $(\chi^2_\nu)^{1/2} \sim 1.2$ and an rms $\sim$7 m s$^{-1}$, correspond to *coplanar* configurations involving two (of three) Jovian planets in 1:1 MMR. The primary parameters ($K$, $e$, $P$, $\omega$, $T_0$) of these fits are given in Table 3 (fits X and XI, respectively). Their planets c and d would have similar periods, but the eccentricities of the two outer planets in 1:1 MMR are significantly different. Unfortunately, these fits are highly unstable. We did not succeed in "stabilizing" them by GAMP; nevertheless, the search was not very extensive, and we suspect that stable solutions involving mutually inclined orbits may exist.

Fit IX (the mathematically best fit found in this paper) yields $(\chi^2_\nu)^{1/2} = 1.08$ and an rms $\sim$6.38 m s$^{-1}$, which indicates an almost "perfect" solution. It could be interpreted as a configuration of the outermost planet accompanying the confirmed giants involved in the 2:1 MMR. Unfortunately, this solution is very unstable due to a large eccentricity of the outermost planet. We tried to refine it with GAMP. In the relevant range of semimajor axes, we found stable solutions, and the one we selected is given as fit VIII in Table 2. Let us note that the stability criterion forces $e_d$ of this solution to a small value $\sim$0.02, which also increases the rms to about 7.35 m s$^{-1}$. The dynamical maps shown in Figure 15 reveal narrow islands of stability in which the solution is found. The MEGNO signature (the left panel of Fig. 16) uncovers a weakly chaotic nature of this solution. Nevertheless, there is no sign of a physical instability over at least 250 Myr (Fig. 16 is for the initial 5 Myr integration period). A peculiarity of this fit is that $e_d$ remains small, in spite of a close proximity to the two larger companions in eccentric orbits. For a comparison with the previously found 1:1 and 2:1 MMR solutions, the synthetic curve of fit VIII is shown in the bottom panel of Figure 14.

TABLE 3
PRIMARY BEST-FIT PARAMETERS OF THREE-PLANET KEPLERIAN MODELS

| | FIT IX HD 82943 (THREE-PLANET) | | | FIT X HD 82943 (THREE-PLANET) | | | FIT XI HD 82943 (THREE-PLANET) | | |
|---|---|---|---|---|---|---|---|---|---|
| PARAMETER | b | c | d | b | c | d | b | c | d |
| $K$ (m s$^{-1}$) | 59.735 | 41.838 | 10.493 | 55.926 | 16.997 | 36.487 | 51.173 | 19.853 | 36.059 |
| $P$ (days) | 219.423 | 442.893 | 937.663 | 219.766 | 417.579 | 445.914 | 219.536 | 418.197 | 449.093 |
| $e$ | 0.398 | 0.141 | 0.580 | 0.403 | 0.712 | 0.061 | 0.437 | 0.683 | 0.210 |
| $\omega$ (deg) | 107.386 | 86.565 | 215.039 | 120.701 | 240.476 | 100.133 | 119.385 | 236.421 | 97.881 |
| $T_p$ (JD-$T_0$) | 1842.338 | 232.810 | 384.940 | 2505.152 | 2141.264 | 3819.642 | 3163.810 | 1722.905 | 1585.272 |
| $(\chi^2_\nu)^{1/2}$ | 1.079 | | | 1.183 | | | 1.180 | | |
| rms (m s$^{-1}$) | 6.37 | | | 6.97 | | | 7.01 | | |
| $V_0$ (m s$^{-1}$) | −3.80 | | | −8.90 | | | −8.65 | | |
| $V_1$ (m s$^{-1}$) | 17.06 | | | 16.99 | | | 16.77 | | |

NOTE.—Primary best-fit parameters of the three-planet Keplerian models found in this paper on the basis of RV measurements of HD 82943 used by Lee et al. (2006). The epoch $T_0$ is JD 2,450,000. The adopted jitter estimate is 4.2 m s$^{-1}$. CORALIE RV measurements are shifted by 8128.598 m s$^{-1}$. All fits are dynamically unstable.

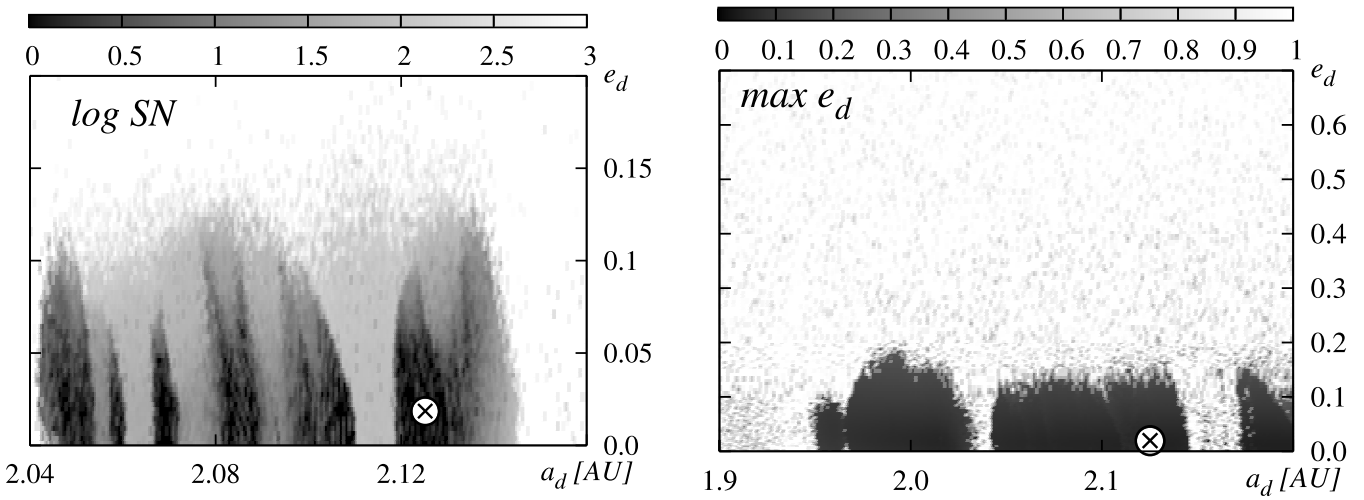


FIG. 15.—Stability maps in the ($a_d$, $e_d$) plane of the HD 82943 system (the resolution is 300 × 120 data points) for the three-planet Newtonian fit VIII (Table 2). The left panel is for the spectral number, log SN. Colors used in the log SN map classify the orbits; black indicates quasi-periodic regular configurations while white indicates strongly chaotic ones. The right panel marked with max $e_d$ is for the maximal eccentricity attained during the integration of the system. The circle marks the parameters of the best-fit solution (fit VIII, Table 2). Note different ranges of the elements in the maps. The integration was conducted for $\sim 6 \times 10^4$ orbital periods of the outermost planet. [*See the electronic edition of the Journal for a color version of this figure*.]

The described results might indicate that our knowledge of the HD 82943 system is still limited, in spite of much effort devoted to study the RV data of the parent star. The currently available measurements permit many qualitatively different orbital solutions that fit the measurements well. Still, the use of stability criterion in the fit process seems to be essential to resolve the degeneracy between very good but strongly unstable Keplerian and Newtonian fits which, as we have shown above, can easily appear.

## 5. CONCLUSIONS

We have demonstrated that the RV measurements for HD 128311 and HD 82943, harboring two-planet systems, can be successfully modeled with two qualitatively different orbital configurations. One is an already recognized configuration corresponding to a 2:1 MMR. We show that these observations are equally well modeled with Trojan pairs of planets (a 1:1 MMR). Both these types of orbital configurations produce very similar periodograms of the RV signal. A common feature of the Trojan solutions for both systems is the possibility for large eccentricities of the orbits, reaching ~0.8. Still, the best-fit Trojan configurations reside in extended zones of rigorously stable quasi-periodic motions. The ease of maintaining stability and the large zones of regular motions may strengthen the hypothesis about the 1:1 MMR configurations.

It is difficult to explain finding two systems in a 1:1 MMR in a sample of only ~20 multiplanet systems. A most promising

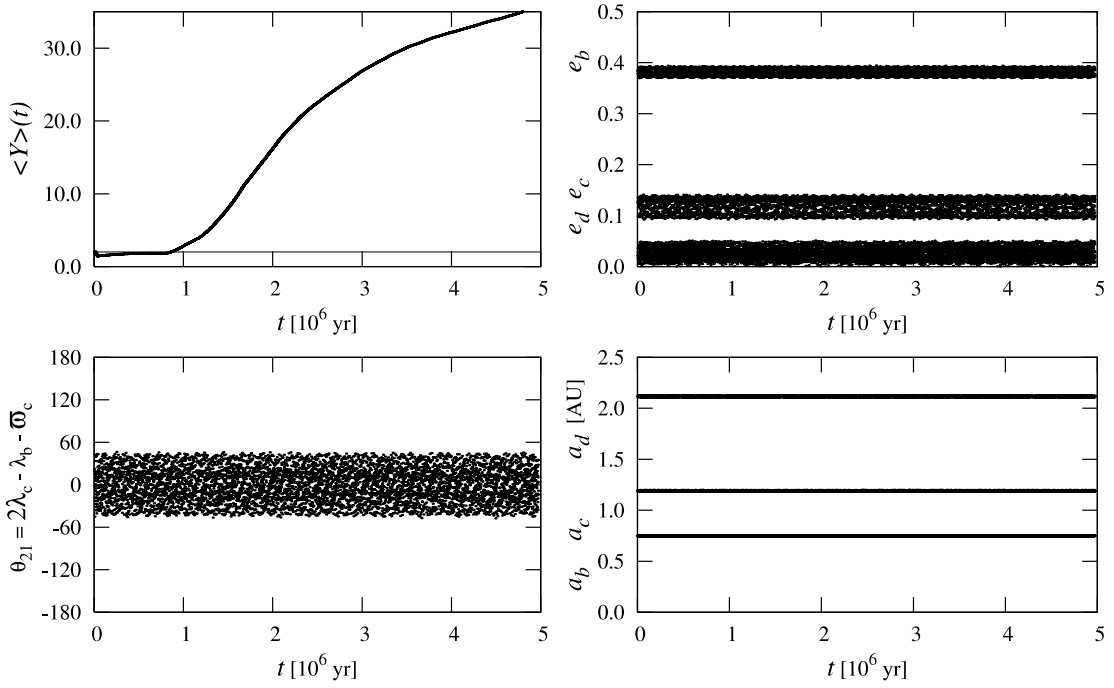


FIG. 16.—Evolution of MEGNO and orbital elements of the three-planet configuration described by fit VIII in Table 2. A slow divergence of MEGNO after ~1 Myr indicates a marginally unstable solution. The evolution of the elements does not change over at least 250 Myr (not shown here). The subsequent panels are for the eccentricities, the critical angle of the 2:1 MMR and the semimajor axes.

mechanism that might produce such a configuration is dynamical relaxation and planetary scattering (Adams & Laughlin 2003). In particular, an argument supporting such a hypothesis for the HD 82943 system is the evidence of a planet engulfment by the parent star (Israelian et al. 2001). That event indicates planetary scattering in the past. However, its effect on the currently observed configuration of the system would be hard to predict. To the best of our knowledge, there are no works that could explicitly explain an inclined 1:1 MMR configuration as a result of a migration. On the other hand, the origin of the 2:1 MMR is a well-recognized problem, as we know of at least four systems presumably involved in such a resonance. Our work demonstrates that the 1:1 MMR configurations can be used to describe the observations of HD 128311 and HD 82943. It is hoped that this will encourage others to study the origin of such systems.

The best-fit Trojan configurations were found using our approach for modeling the RV data, which incorporates a stability indicator. For this purpose, we use a formal KAM criterion that is closely related to the physical behavior of a planetary system. This criterion generalizes the max $e$ and max $\theta$ maps. Still, these maps help us to determine the character of motions; e.g., the type of corotation of the apsides. Obviously, all three indicators are strictly related. Presumably, the stability maps would change if the model of motion included the relativistic and tidal interactions with the star. Although these factors are orders of magnitude smaller than the leading gravitational interactions, their influence might change the overall stability picture of the systems. Our work on this subject is ongoing.

*Note added in manuscript*.—Recently, Tinney et al. (2006) announced a new multiplanet system around HD 73526. The authors explain the RV variability of this star by the presence of two planetary companions involved in the 2:1 MMR. Following the discovery team, we adopted a jitter of $\sim$3.3 m s$^{-1}$ and the mass of the star as 1.08 $M_{\odot}$. Using GAMP, we also found stable 1:1 MMR configurations with an rms comparable with that of the best dynamical fit quoted by Tinney et al. (2006), $\sim$7.9 m s$^{-1}$. For example, the configuration with the astrocentric osculating elements ($m$ [$M_J$], $a$ [AU], $e$, $i$ [deg], $\Omega$ [deg], $\omega$ [deg], and $M$ [deg]) at the date of the first observation JD 2,450,1212.1302: (8.092, 1.058, 0.488, 28.067, 168.17, 169.63, and 48.68) and (8.765, 1.060, 0.221, 53.963, 0.00, 209.42, and 184.92) for the two planets, respectively, and $V_0 = -78.64$ m s$^{-1}$ yields an rms $\sim$7.71 m s$^{-1}$ and $(\chi^2_\nu)^{1/2} \sim 1.18$. The eccentricities of both planets are moderate compared to the two systems analyzed in this work. The 1:1 configuration is located in an extended stability zone in the ($a_b$, $a_c$) plane, similar to HD 82943 and HD 128311. Other stable solutions with larger masses $\sim$11 $M_J$ exist as well.

We appreciate discussions with Sylvio Ferraz-Mello and his help with obtaining the RV data of the HD 82943 system. We thank Man Hoi Lee for a detailed review and critical remarks that improved the manuscript and for providing the full set of RV measurements of HD 82943. This work is supported by the Polish Ministry of Education and Science, grant 1P03D 021 29. M. K. is also supported by NASA through grant NNG04GM62G.

## APPENDIX

Here we discuss the problem of a proper choice of the stability indicator in a GAMP-like fitting code. We analyze two 1:1 initial conditions for the HD 82943 system that are marked in the stability maps (Fig. 8, *top row;* one is our best-fit 1:1 MMR configuration). Let us recall that the calculations of SN were conducted over $6 \times 10^4$ orbital periods of the planets (of about $6 \times 10^4$ yr). Apparently, both initial conditions are localized in an extended resonance zone. Figure 17 (*top row*) illustrates the temporal MEGNO, $Y(t)$, as a function of time but computed over a much longer time span, $2.5 \times 10^5$ orbital periods. For the best-fit solution, the behavior of $Y(t)$ (oscillations

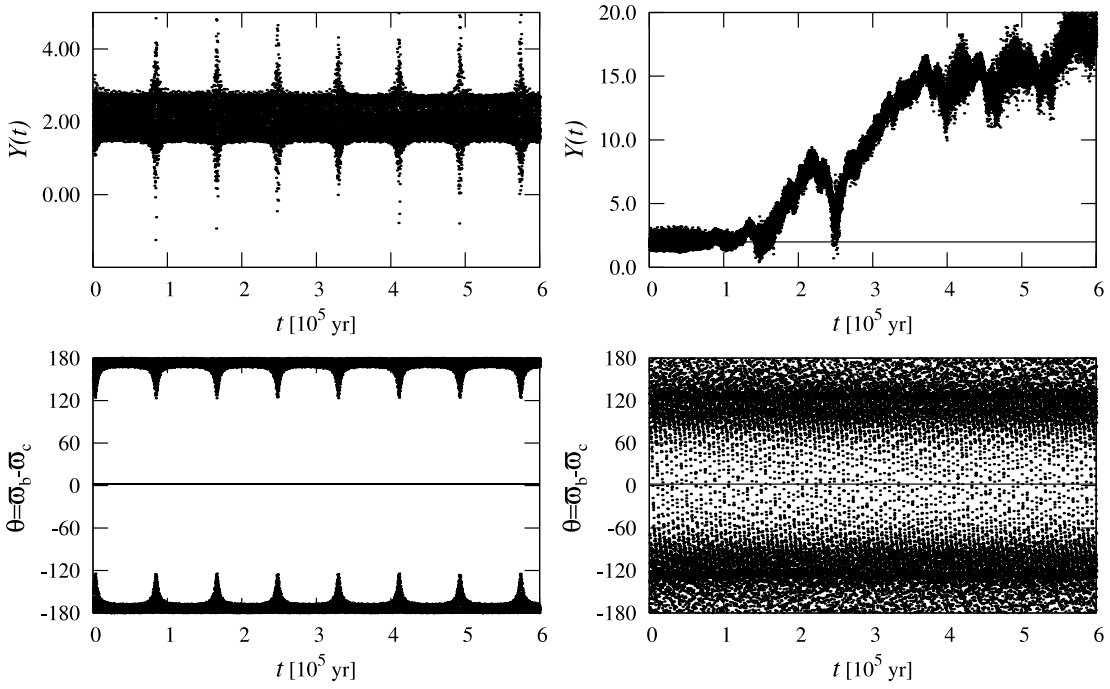


FIG. 17.— Left column is for the evolution of MEGNO, $Y(t)$, and $\theta$ for the best-fit 1:1 MMR solution (fit IV, Table 1) for HD 82943. The right column is for the initial condition marked with a diamond in Fig. 8.

about 2) corresponds to a strictly quasi-periodic system, while a slow divergence of this indicator can be observed for the modified initial condition (marked with a diamond in the SN map, Fig. 8). It indicates that, in this case, the system is in fact weakly chaotic (the Lyapunov exponent is relatively small, $\sim 10^{-5}\,\mathrm{yr}^{-1}$). An inspection of the max $\theta$ map for this initial condition reveals that $\theta$, in this case, circulates (Fig. 8 and Fig. 17, *right column*), but on average, the apsides are anti-aligned, and this helps to maintain the stability. It means that max $\theta$ would not be a good choice as a stability indicator. Nevertheless, it is a valuable tool for resolving the complex structure of the resonance.

## REFERENCES


Adams, F. C., & Laughlin, G. 2003, Icarus, 163, 290
Arnold, V. I. 1978, in Graduate Texts in Mathematics, Mathematical Methods of Classical Mechanics (New York: Springer)
Beaugé, C., & Michtchenko, T. A. 2003, MNRAS, 341, 760
Butler, R. P., Marcy, G. W., Vogt, S. S., Fischer, D. A., Henry, G. W., Laughlin, G., & Wright, J. T. 2003, ApJ, 582, 455
Charbonneau, P. 1995, ApJS, 101, 309
Ferraz-Mello, S., Michtchenko, T. A., & Beaugé, C. 2005, ApJ, 621, 473
Goździewski, K., & Konacki, M. 2004, ApJ, 610, 1093
Goździewski, K., Konacki, M., & Maciejewski, A. J. 2003, ApJ, 594, 1019
———. 2005, ApJ, 622, 1136
———. 2006, ApJ, 645, 688
Goździewski, K., & Maciejewski, A. 2001, ApJ, 563, L81
Goździewski, K., & Migaszewski, C. 2006, A&A, 449, 1219
Israelian, G., Santos, N. C., Mayor, M., & Rebolo, R. 2001, Nature, 411, 163
Ji, J., Kinoshita, H., Liou, L., Nakai, H., & Li, G. 2003, ApJ, 591, L57
Ji, J., Liu, L., Kinoshita, H., Zhou, J., Nakai, H., & Li, G. 2003, Celest. Mech. Dyn. Astron., 87, 113
Kley, W. 2003, Celest. Mech. Dyn. Astron., 87, 85
Kley, W., Peitz, J., & Bryden, G. 2004, A&A, 414, 735
Laughlin, G., & Chambers, J. E. 2001, ApJ, 551, L109
———. 2002, AJ, 124, 592
Lecar, M., Franklin, F. A., Holman, M. J., & Murray, N. J. 2001, ARA&A, 39, 581
Lee, M. H. 2004, ApJ, 611, 517
Lee, M. H., Butler, R. P., Fischer, D. A., Marcy, G. W., & Vogt, S. S. 2006, ApJ, 641, 1178
Lee, M. H., & Peale, S. J. 2002, ApJ, 567, 596
———. 2003, ApJ, 592, 1201
Lissauer, J. J. 1999, Rev. Mod. Phys., 71, 835
Marcy, G., Butler, R., Fischer, D., Vogt, S., Lissauer, J., & Rivera, E. 2001, ApJ, 556, 296
Mayor, M., Udry, S., Naef, D., Pepe, F., Queloz, D., Santos, N. C., & Burnet, M. 2004, A&A, 415, 391
Michtchenko, T., & Ferraz-Mello, S. 2001, AJ, 122, 474
Nauenberg, M. 2002, AJ, 124, 2332
Press, W. H., Teukolsky, S. A., Vetterling, W. T., & Flannery, B. P. 1992, Numerical Recipes in, C. The Art of Scientific Computing (2nd ed.; Cambridge: Cambridge Univ. Press)
Psychoyos, D., & Hadjidemetriou, J. D. 2005, Celest. Mech. Dyn. Astron., 92, 135
Rivera, E. W., & Lissauer, J. J. 2001, ApJ, 558, 392
Thommes, E. W., & Lissauer, J. J. 2003, ApJ, 597, 566
Tinney et al. 2006, ApJ, 647, 594
Vogt, S. S., et al. 2005, ApJ, 632, 638
Wright, J. T. 2005, PASP, 117, 657